

See discussions, stats, and author profiles for this publication at: <https://www.researchgate.net/publication/255765364>

A novel strategy for surface treatment on hematite photoanode for efficient water oxidation

ARTICLE *in* CHEMICAL SCIENCE · NOVEMBER 2012

Impact Factor: 9.21 · DOI: 10.1039/C2SC20881D

CITATIONS

36

READS

32

7 AUTHORS, INCLUDING:



Lifei Xi

Helmholtz-Zentrum Berlin

25 PUBLICATIONS 580 CITATIONS

[SEE PROFILE](#)



Phong D Tran

University of Science and Technology of Han...

39 PUBLICATIONS 1,217 CITATIONS

[SEE PROFILE](#)



James Barber

Imperial College London

520 PUBLICATIONS 22,358 CITATIONS

[SEE PROFILE](#)



Joachim SC Loo

Nanyang Technological University

163 PUBLICATIONS 3,412 CITATIONS

[SEE PROFILE](#)

Electronic Supplementary Information (ESI)

A novel strategy for surface treatment on hematite photoanode for efficient water oxidation

Lifei Xi,^a Sing Yang Chiam,^b Wai Fatt Mak,^a Phong D. Tran,^c James Barber,^{a,d,e*} Joachim Say Chye Loo^{a*} and Lydia Helena Wong^{a*}

^a School of Materials Science and Engineering, Nanyang Technological University, Singapore, 639798

E-mail: j.barber@imperial.ac.uk, Joachimloo@ntu.edu.sg, Lydiawong@ntu.edu.sg

^b Institute of Materials Research and Engineering (IMRE), Agency of Science, Technology, and Research (A*Star), 3 Research Link, 117602, Singapore.

^c Energy Research Institute @ NTU, Nanyang Technological University, 50 Nanyang Drive, Research Techno Plaza, X-Frontier Block, Level 5, Singapore 637553

^d Division of Molecular Biosciences Imperial College London, London, SW7 2AZ, UK

^e BioSolar Laboratory, Department of Material Sciences and Chemical Engineering, Polytechnic of Torino, Corso Duca degli Abruzzi, 24, 10129, Torino, Italy

* CORRESPONDING AUTHOR, E-mail: j.barber@imperial.ac.uk, Joachimloo@ntu.edu.sg, Lydiawong@ntu.edu.sg

1. Experiment details

1.1 Synthesis of FeOOH nanorod arrays. Hematite nanorod arrays were grown on a fluorine-doped tin oxide (FTO, Nippon Sheet Glass Co Ltd, 15 Ω/\square) substrates by a modified procedure based on our previous work.¹ In typically, a 10 mL aqueous solution containing 1.5 mmol FeCl₃·6H₂O (Sigma, ACS reagent 97%) and 1.5 mmol urea (Sigma, 98%) was transferred into a 20 mL Teflon-lined autoclave and four substrates (1 cm x 2.5 cm) were placed at an angle facing the wall of the autoclave. After 10 hr of reaction at 100 °C, a uniform layer of yellow FeOOH film was formed on the FTO substrate. The substrates were thoroughly rinsed in DI water to remove any residue ions and surface precipitation.

1.2 Sn (IV) aqueous solution treatment on FeOOH nanorod arrays. A 70 μ L of SnCl₄·5H₂O (Sigma-Aldrich, 98 %) aqueous solutions were freshly prepared and dropped on the above wet FeOOH film. A series of Sn (IV) aqueous solutions was studied, including 0, 5, 20, 60, 90 mM.

The substrates were kept horizontal for at least 5 min at room temperature before heated up inside a box furnace (Model: LE 6/11/P300, Nabertherm, Germany). The substrates were subsequently slowly heated up to 750 °C with a heating rate of 4°C/min. They were held at this temperature for 30 min.

1.3 Characterization and measurements.

Morphology of samples was characterized by FESEM (JEOL, JSM-7600F, 5kV) and TEM. Scanning TEM (STEM) image, mappings and line scans were carried out using JEOL 2100F microscopes with a field emission gun and the acceleration voltage for both microscopes was 200 kV. Diffuse reflectance ultraviolet-visible (UV-Vis) absorption spectra of the films were obtained using an Agilent Cary series UV-Vis-NIR spectrophotometer (Model: Cary 500) equipped with an external diffuse reflectance accessory (DRA-2500). The diameter of integrating sphere was 150 mm. The XPS measurements were carried out in an ultrahigh vacuum VG ESCALAB 220i-XL system equipped with a monochromatic Al Ka (1486.6 eV) source for XPS. PEC measurements were performed using CHI 660D working station (CH Instruments, Inc.) in a three-electrode electrochemical system with 1 M NaOH (pH=13.6) electrolyte. Platinum mesh and Ag/AgCl were employed as counter and reference electrodes, respectively. The working surface area was 0.2 cm². The light source was simulated sunlight from a 150 W xenon solar simulator (67005, Newport Corp.) through a solar filter with a measured intensity equivalent to standard AM1.5 sunlight (100 mW/cm²) at the sample face. 1 M NaOH electrolyte or 1 M NaOH with 0.5 M H₂O₂ electrolyte were degassed by purging N₂ gas for 10 min. IPCE characteristics were measured with a xenon light source (MAX-302, Asahi Spectra Co. Ltd.) coupled with a monochromator (CMS-100, Asahi Spectra Co. Ltd.) from 305 to 630 nm, at a potential of 1.23 V vs RHE. A Si photodiode (Bentham, DH-Si) with known IPCE was used to calculate the IPCE of the pure hematite and Sn (IV) treated hematite photoanodes. A source meter (Keithley Instruments Inc., Model: 2400) was used to measure the photocurrent of Si diode. The working station (CHI 660D, CH Instruments, Inc.) mentioned above was used to measure the photocurrent of samples. The equation for IPCE calculation was as following:

$$IPCE = (photocurrent\ of\ sample * IPCE\ of\ Si\ diode) / photocurrent\ of\ Si\ diode.$$

The electrochemical impedance spectroscopy (EIS) measurements were carried out using an automated potentiostat (Solartron-analytical, 1470E) coupled with a frequency response analyzer (Solartron-analytical, 1255B) in a three-electrode electrochemical system. Reference electrode and counter electrode were same as that of PEC measurements. For Mott-Schottky plots, the EIS data were measured with a sinusoidal voltage perturbation of 10 mV amplitude between 100 KHz to 100 Hz scanned from -1.0 V to 1.0 V in dark. A typical Mott-Schottky plot was extracted at 1 KHz. The analysis of gaseous product under irradiation was performed using a gas chromatograph (GC) (Agilent 7890A). The gas was manually injected inside GC. The potential of the working electrode was controlled at 1.23 V vs RHE in a three-electrode system. The active area was 1 cm². Other conditions are same as that of PEC measurements.

1.4 Supporting information for calculations:

1.4.1 Charge separation and injection yields:

The calculations were followed a reported method.^{2,3} The equations used were as following:

$$J_{2}^{H_2O} = J_{\text{absorbed}} \times \eta_{\text{charge separation}} \times \eta_{\text{charge injection}} \quad (1)$$

$$J_{2}^{H_2O} = J_{\text{absorbed}} \times \eta_{\text{charge separation}} \quad (2)$$

where $J_{2}^{H_2O}$ is the photocurrent at 1.23 V vs RHE, J_{absorbed} is photon absorption expressed as a current density after integrated with AM1.5G solar spectrum, $\eta_{\text{charge separation}}$ is the charge separation yield of the photogenerated carries, and $\eta_{\text{charge injection}}$ is the charge injection yield or the interfacial hole injection yield which is equal to $J_{2}^{H_2O} / J_{2}^{H_2O}$.³

1.4.2 The active surface area (S_a) was calculated as following:

$$S_a = S_{\text{planar}} + S_{\text{nanorods}}$$

Where S_{planar} is the planar area on the electrode where no nanorod occupied and which is equal to $(S_t - n \pi R^2/4)$, n is the number of nanorod/cm² (1.2×10^{10}) which is calculated based on Fig 2d in the main text, S_t is the test area of plane electrode (1 cm²), R is the diameter of nanorod (50 nm), S_{nanorods} is equal to $n(\pi R^2/4 + \pi R h)$ and h is the length of nanorod (500 nm). S_a was found around 10 times higher than S_t .

1.4.3 Electron donor density (N_D) and space charge region width (W):^{4, 5}

$$1/C^2 = 2(V - V_{FB} - KT/e_0) / \epsilon_0 \epsilon N_D S^2$$

$$W = [2\epsilon_0 \epsilon (V - V_{FB} - KT/e_0) / e_0 N_d]^{1/2}$$

Where C is the space charge capacitance (F), ϵ_0 is the permittivity of vacuum, ϵ is the dielectric constant of hematite (80), V is the applied potential (V), V_{FB} is the flat band potential (0.48V vs

RHE), S is the surface area (cm^2), KT/e_0 is a temperature-dependent correction term (0.026 V at 25 °C), e_0 is the elemental charge and N_d is the dopant density (cm^{-3}) which can be determined by plotting $1/C^2$ as a function of the applied potential. At applied potential of 1.23V vs RHE and electron density of 6×10^{20} , 12×10^{20} and $29 \times 10^{20} \text{ cm}^{-3}$, the space charge widths (W) have been calculated to be 3.3 nm, 2.1 nm and 1.5 nm which are far smaller than radius of nanorods (25 nm).

1.4.4 Meaning of ideality factor: The semiconductor/electrolyte is analogous to a “Shottky barrier”.⁴ The dark current of electrode is given by

$$I = I_D [\exp(e_0V/nKT) - 1]$$

Where I is the dark current density, I_D is the dark saturation current, e_0 is the elemental charge, V is the applied voltage, n is the ideality factor, k Boltzmann constant and T is the temperature in kelvin. The ideality factor which determines how closely the diode follows the ideal diode equation is determined from the slope of the exponential regime of the dark I - V curves on a semi-logarithmic plot (the slope gives e_0/nKT).^{4, 6} It contains important information on the recombination processes and thus is a powerful tool for examining the recombination in solar cells and photoelectrochemical cells. In general, the ideality factor of 2 is an indication of electron transfer across semiconductor/electrolyte interface, which depends on Butler-Volmer equation.⁷ A larger ideality factor (bigger than 2) indicate a higher chance of recombination at interface. Since hematite is n-type semiconductor, the forward bias region of the I - V curve is at negative potential. At this region, the electron transfer from the conduction band across the hematite/electrolyte can be studied. It showed the effect of Sn (IV) treatment.

2. Supporting figures and captions.

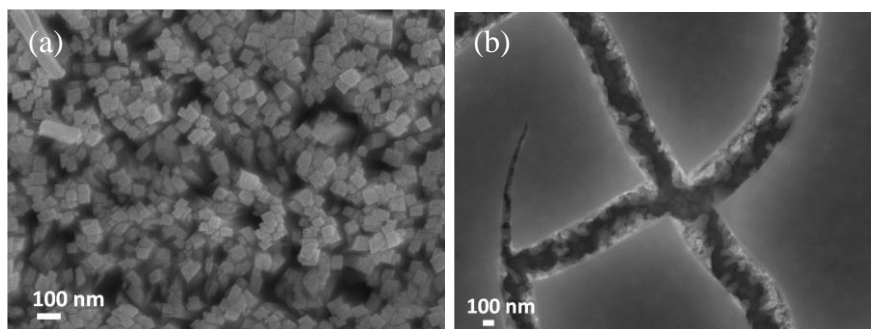


Fig. S1 SEM images of (a) FeOOH nanorod array after hydrothermal reaction at 100°C for 10 hr and (b) hematite treated with 90 mM Sn (IV) solution.

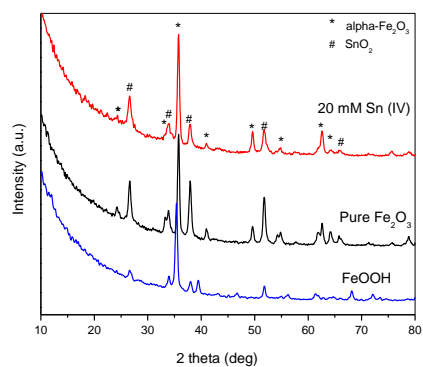


Fig. S2 XRD patterns of FeOOH, hematite nanorod arrays on FTO without and with 20 mM Sn (IV) treatment after annealed at 750 °C for 30 min. The * denotes Fe₂O₃ (JCPDS 33-0664) and # denotes SnO₂ (JCPDS 46-1088), respectively.

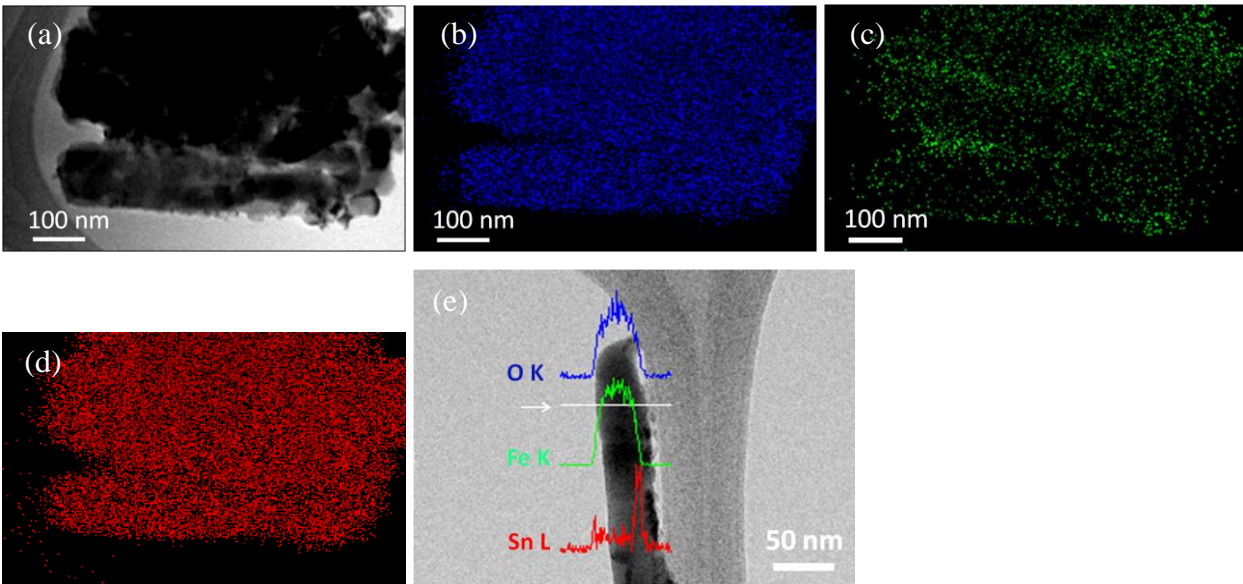
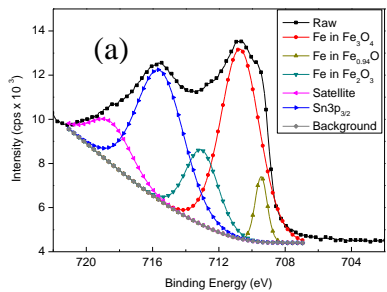


Fig. S3 (a) STEM image of hematite nanorods after treated with 20 mM Sn (IV). (b) – (e) Maps for elemental Fe, Sn and O, and (e) EDAX line-scan for a single hematite nanorod after treated with 20 mM Sn (IV).



(b)	Sn % (molar ratio)
pure	6.99
5mM	13.63
20 mM	34.87

Fig. S4 (a) XPS spectra of fitted Fe 2p scan for 20 mM Sn (IV) treated sample. (b) XPS quantitative analysis of Sn molar ratio ($\text{Sn}/(\text{Sn}+\text{Fe})$) for different samples.

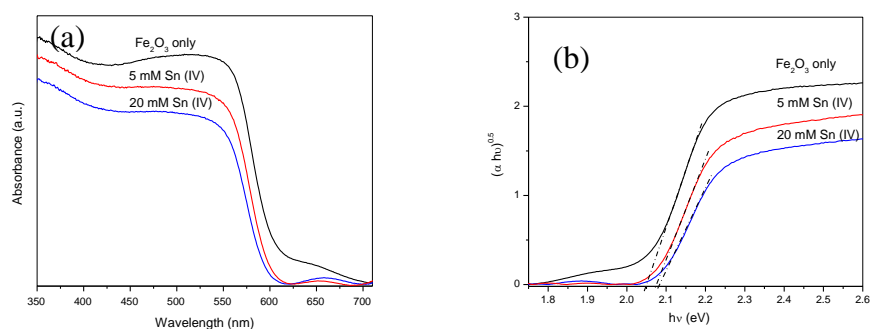


Fig. S5 (a) Diffuse reflectance UV-Vis absorption and (b) Tauc-Plots of films of hematite with and without Sn (IV) treatment.

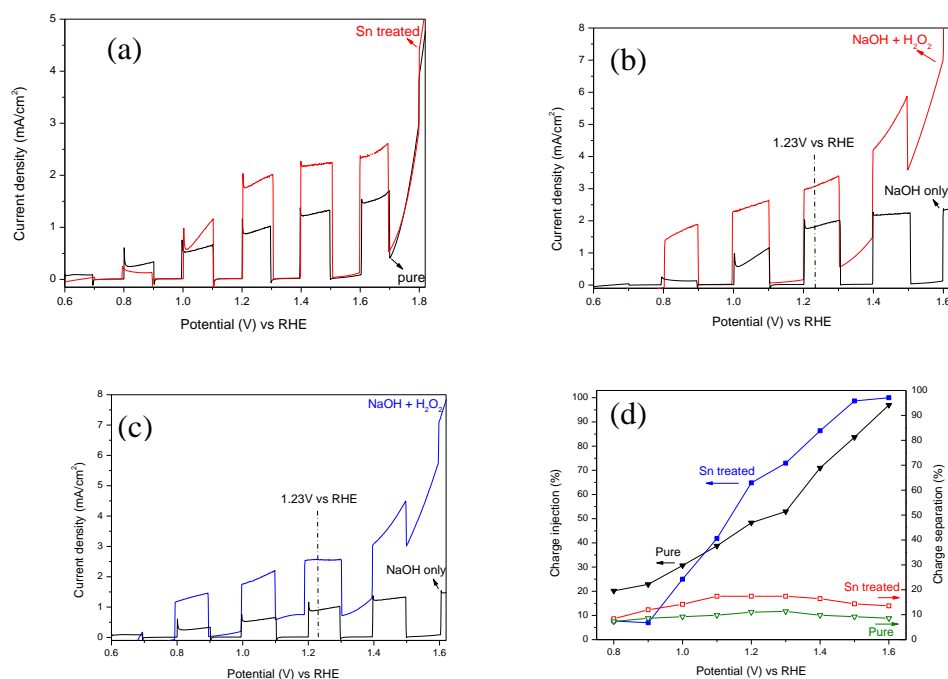


Fig. S6 (a) Chopped I-V curves of hematite photoanode with 20 mM Sn (IV) treatment. (b) Chopped I-V curves of hematite treated with 20 mM Sn (IV) tested in 1 M NaOH and 1M NaOH-0.5 M H_2O_2 . (c) Chopped I-V curves of the pristine hematite tested in 1 M NaOH and 1M NaOH-0.5 M H_2O_2 . (d) Charge separation and injection yields of the pristine hematite and hematite treated with Sn (IV) solution. The calculations for charge separation and injection yields were followed a reported method.^{2,3}

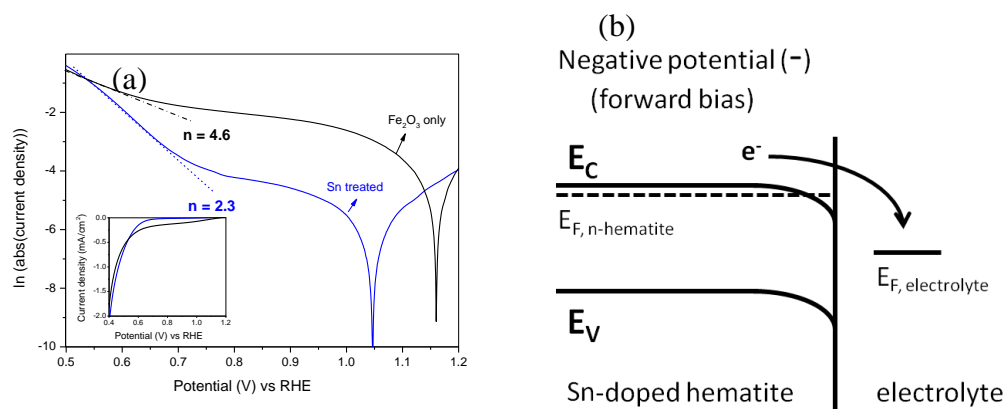


Fig. S7 (a) Local ideality factor extracted from the dark I-V curves (inset) with and without 20 mM Sn (IV) treatment. Electrolyte solution: an aqueous solution of 50 mM of $\text{K}_4\text{Fe}(\text{CN})_6$ (Sigma, >99.99%), 5 mM $\text{K}_3\text{Fe}(\text{CN})_6$ (Sigma, 99%) and 200 mM KCl in a pH6.9 phosphate buffer solution (0.1M). Scan rate: 10 mV s^{-1} . (b) Band alignment of Sn-doped hematite/electrolyte under forward bias and dark conditions.

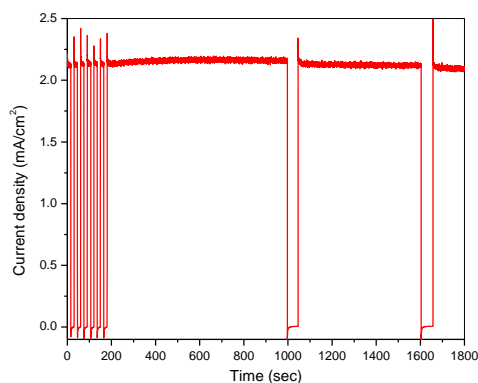


Fig. S8 Photocurrent stability profile of 20 mM Sn (IV) treated hematite photoanode.

References

1. Mulmudi, H. K.; Mathews, N.; Dou, X. C.; Xi, L. F.; Pramana, S. S.; Lam, Y. M.; Mhaisalkar, S. G. *Electrochem. Commun.* **2011**, *13*, 951.
2. Dotan, H.; Sivula, K.; Gratzel, M.; Rothschild, A.; Warren, S. C. *Energy Environ. Sci.* **2011**, *4*, 958.
3. Hisatomi, T.; Dotan, H.; Stefik, M.; Sivula, K.; Rothschild, A.; Gratzel, M.; Mathews, N. *Adv. Mater.* **2012**, *24*, 2699.

4. R. van de Krol and M. Gratzel (eds), Photoelectrochemical Hydrogen Production, Electronic Materials: Science & Technology 102, Springer Science + Business Media, LLC 2012.
5. Yu, Q.; Cao, C. B. *J. Nanosci. Nanotechnol.*, **2012**, *12*, 3984-3989.
6. Okumura, T.; Kaneshiro, C. Electronics and Communications in Japan, Part 2, 1999, 82, 13.
7. Soga, T., Nanostructured Materials for Solar Energy Conversion, Elsevier, 2006, 90.